Università degli studi di Udine

Altered dynamics of brain connectivity in major depressive disorder at-rest and during task performance

(Article begins on next page)

20 April 2024

Altered dynamics of brain connectivity in major depressive disorder at-rest and during task performance

Fabio Sambataro, MD, PhD [a]; Eleonora Visintin [b]; Nadja Doerig [c]; Janis Brakowski, MD [d];

Martin Grosse Holtforth, PhD [e]; Erich Seifritz, MD [d,f,g]; Simona Spinelli, PhD [f,g, h]

Author affiliations:

[a] Department of Experimental and Clinical Medical Sciences, University of Udine, Udine, Italy.

[b] Neuroscience and Brain Technologies, Istituto Italiano di Tecnologia, Genova, Italy.

[c] Clinical Center for Psychosomatics, Sanatorium Kilchberg AG, Zurich, Switzerland.

[d] Department of Psychiatry, Psychotherapy and Psychosomatics, Psychiatric Hospital, University

of Zurich, Switzerland.

[e] Department of Psychology, University of Bern, Switzerland.

[f] Zurich Center for Integrative Human Physiology, University of Zurich, Switzerland.

[g] Neuroscience Center, University and ETH Zurich, Switzerland.

[h] Preclinical Laboratory for Translational Research into Affective Disorders, Department of

Psychiatry, Psychotherapy and Psychosomatics, Psychiatric Hospital, University of Zurich,

Switzerland.

Correspondence:

Fabio Sambataro, MD, PhD

Department of Experimental and Clinical Medical Sciences,

University of Udine,

P.le Kolbe 3

I-33100 Udine, Italy

email: fabio.sambataro@uniud.it

Tel.: +39 0432 559494

Simona Spinelli, PhD

Preclinical Laboratory for Translational Research into Affective Disorders,

Department of Psychiatry, Psychotherapy and Psychosomatics,

Psychiatric Hospital, University of Zurich,

August Forel-Strasse 7, CH-8008 Zurich, Switzerland

Tel. +41 44 634 8923

e-mail: spinellisimona@gmail.com

Word Count Abstract: 192

Word Count Main Text: 5136

Abstract

Major depressive disorder (MDD) has been associated with alterations in several functional brain networks. Previous studies investigating brain networks in MDD during the performance of a task have yielded inconsistent results with the function of the brain at rest. In this study, we used functional magnetic resonance imaging at rest and during a goal-directed task to investigate dynamics of functional connectivity in 19 unmedicated patients with MDD and 19 healthy controls across both experimental paradigms. Patients had spatial differences in the default mode network (DMN), in the executive network (EN), and in the dorsal attention network (DAN) compared to controls at rest and during task performance. In patients the amplitude of the low frequency (LFO) oscillations was reduced in the motor and in the DAN networks during both paradigms. There was a diagnosis by paradigm interaction on the LFO amplitude of the salience network, with increased LFO amplitude change between task and rest in patients relative to controls. Our findings suggest that the function of several networks could be intrinsically affected in MDD and this could be viable phenotype for the investigation on the neurobiological mechanisms of this disorder and its treatment.

1. Introduction

Major depressive disorder (MDD) is a severe psychiatric disorder with a lifetime prevalence of 10 to 20% in the general population and a significant risk for chronicity and disability (DeRubeis et al., 2008). Altered structure and/or function of a large number of brain regions has been associated with MDD, thus suggesting that the pathophysiology of depression entails multiple brain circuits (Pandya et al., 2012).

Resting-state functional magnetic resonance imaging (RS-fMRI) is a valuable method to understand how functional alterations in different brain regions are related to intrinsic networks (INs, (Biswal et al., 2010)). Previous evidence from RS-fMRI indicates that spatially separated brain regions show temporal correlations in their blood-oxygen-level-dependent (BOLD) signal (Biswal et al., 1995). These synchronous neuronal signal fluctuations are considered to reflect functional connectivity (FC) of segregated neuro-anatomical INs (Fox and Raichle, 2007; Seeley et al., 2007). Based on their spectral profile, low frequency oscillations (LFO) are those spontaneous neuronal signal fluctuations with frequency <0.08 Hz (Buzsaki and Draguhn, 2004). BOLD LFOs are thought to originate in the gray matter and therefore associated with the neural processes underlying FC of the brain networks (Zuo et al., 2010).

In MDD alterations of multiple INs have been reported (Hamilton et al., 2011; Marchetti et al., 2012; Northoff et al., 2011; Pizzagalli, 2011), including the default mode network (DMN), which comprises a set of brain regions more engaged during rest relative to goal-oriented tasks (Raichle and Snyder, 2007). Whole brain functional connectivity patterns at rest could be able to differentiate with high confidence patients with MDD from healthy controls (Zeng et al., 2012). Interestingly, the patterns of FC with highest discriminative power were located in multiple networks, including the DMN. More recently, two meta-analyses and a systematic review of RS-fMRI studies agreed upon a role of functional alterations in multiple networks in MDD including the DMN, and dorsal attention network

(DAN), the executive network (EN), and the salience network (SN) (Kaiser et al., 2015; Sundermann et al., 2014; Wang et al., 2012b). Furthermore, we and others have demonstrated altered LFOs during resting state in patients with MDD (Guo et al., 2012; Sambataro et al., 2013; Wang et al., 2016). Notably, temporal network dysfunctions are already present in patients at the first MDD episode and medication naïve (Liu et al., 2013). Widespread alterations of LFOs of resting state networks have been described in multiple brain circuits including the salience, the DAN, the DMN (Guo et al., 2012; Sambataro et al., 2013; Wang et al., 2016), and the motor networks (Wang et al., 2016).

Neuroimaging literature implicates altered network function in MDD also during the performance of a task, including those networks associated with emotional, cognitive (Roiser et al., 2012), and motor processing (Liberg and Rahm, 2015). Nonetheless, the extent to which spatial and temporal characteristics of intrinsic networks are also altered during task performance has not been extensively studied. A recent meta-analysis on the brain activation differences in task-based fMRI concluded that MDD was associated with a pattern of functional activation abnormalities in cortico-limbic/cortico-striatal circuits rather than with regions of the DMN (Graham et al., 2013), thus showing a poor spatial overlap between task-based and RS-fMRI findings in MDD (Sundermann et al., 2014).

This discrepancy could be explained by the paucity of studies investigating connectivity patterns both at rest and during task performance in the same individuals with MDD. Furthermore, results' inconsistency could arise from different analytical methods used to analyze RS- and task-fMRI data. In particular, the use of seed-based analysis which estimates connectivity between *a priori* selected regions-of-interest (seeds) and the rest of the brain (Wang et al., 2012b) could explain the over-representation of DMN alterations in RS-fMRI studies. Spatial and statistical features in the selection of an *a priori* seed per se could also cause an observational bias (Cole et al., 2010). Also, as a single seed can be analyzed at the time, only a limited number of networks are investigated in each analysis.

5

Alternative to this approach, independent component analysis (ICA), a model-independent multivariate statistical analysis, can extract spatially independent and temporally synchronous activity patterns in brain regions, which represent FC (Calhoun et al., 2001). First, this approach allows the estimation of spatial patterns of FC that fluctuate over time; second, FC patterns are estimated across multiple brain networks at once thus avoiding a observational bias in network selection (Veer et al., 2010). To date, few fMRI studies have employed ICA to investigate functional abnormalities in MDD during task (Vasic et al., 2009) or at-rest (Greicius et al., 2007; Sambataro et al., 2013; Shi et al., 2015; Veer et al., 2010; Zhu et al., 2012). Of these studies, only one conducted a comprehensive network analysis. Veer *et al.* (2010) identified 13 INs at-rest, 3 of which showed reduced FC in unmedicated patients with MDD compared to healthy controls. These networks included a DAN, a visual network, and an affective network involved in emotional regulation, but no significant differences were found in the DMN (Veer et al., 2010). However, whether the functional abnormalities of the INs in MDD are similar at-rest and during task remains unclear.

In this study, we set out to investigate the dynamics of network function across different experimental paradigms (at rest and during a cognitive task) in unmedicated patients with MDD and healthy volunteers. Based on this literature, we hypothesized that: 1) patients with MDD would show consistent alterations in patterns of FC of the DMN, the EN, the DAN, and the SN both at rest and during a goal directed processing; 2) the temporal oscillations of these networks would be altered in the low frequency range. To this aim, we studied FC and spectral properties of multiple brain networks, and their between network connectivity in the same subjects with MDD while at rest and during the performance of a low demanding cognitive task. To reduce the risks of observational biases and false positive results, we used a hierarchical multivariate approach (Allen et al., 2011). With the multi-paradigm approach we aimed at identifying not only those diagnosis-related changes that are associated with paradigm performance, but also those that are independent from the experimental

conditions and therefore more robust. Also, we wanted to assess whether diagnosis

modulated network function depending on the experimental condition.

2. Methods

2.1. Participants

Nineteen unmedicated patients with MDD and nineteen healthy controls without any

psychiatric, neurologic, or medical illness (all Caucasians) completed the study (see also

Supplemental Information). Groups did not differ for gender distribution, age, years of

education and performance in a motion prediction task. Thirteen patients with MDD were

medication naïve. All the other patients had been off-medication for at least six weeks

before the study (four of them were under antidepressant treatment, and for other two past

treatment information was not available). Exclusion criteria for both groups included age

<18 or >65 years, current presence of psychosis as assessed by SCID-I interview or self-

reported past history of psychosis or bipolar disorder, major medical or neurological illness;

current drug or alcohol abuse, MRI contraindications. Inclusion in the MDD group was

contingent on a diagnosis of current MDD based on a SCID-I semi-structured interview

(DSM-IV-TR). Six subjects with MDD had comorbid anxiety disorders (Supplemental

Information). The study was approved by the University of Zurich's Institutional Review

Board, and all subjects gave written informed consent. They were paid 25 CHF/hour and the

gains related to the experimental task.

2.2. MRI Imaging

2.2.1 Image Acquisition

Images were acquired on a Philips Achieva 3-Tesla whole-body MRI unit equipped with an

eight-channel head coil using a sensitivity encoded single shot echo-planar sequence

(acceleration factor R=2). A T1-weighted gradient echo sequence (turbo field echo) with a

spatial resolution of 0.94×0.94×1.00mm^3 (matrix: 240×240pixels; 160slices), field of view=240×240mm^2, TE=3.7ms, TR=8.06ms, and flip angle=8° was applied. For the acquisition of the functional images, the subjects were told to lie still in the scanner with their eyes closed and let their minds wander (Logothetis et al., 2009; Northoff et al., 2010); 300 functional images were collected in a single 10-min run. The following parameters were used: TR=2000ms, TE=30ms, flip angle=75°, ascending acquisition order, 80×80voxel matrix and voxel size=3×3×4mm^3.

Thirty-six contiguous axial slices were placed along the anterior-posterior commissure plane covering the entire brain. The first four acquisitions were discarded due to T1 saturation effects. Six hundred images of functional imaging data during the performance of a motion prediction task were acquired in the same session with similar scanning parameters. The task is described in details in (Späti et al., 2014) and the Supplemental Information. The acquisition of resting-state and task data was always separated by about 10-min during which we acquired structural data. Structural MRI scans were screened by an experienced neuroradiologist for structural brain abnormalities and other incidental lesions. Nonetheless, we did not exclude subjects for this reason.

2.2.2. Image Preprocessing

Functional data and structural were preprocessed and analyzed using Statistical Parametrical Mapping (SPM8; http://www.fil.ion.ucl.ac.uk; see supplementary information for details). To avoid a bias following a different number of volumes between rest and task fMRI acquisition, we limited our analysis to the first 300 volumes of the task scan. Also, task fMRI included both trials and inter-trial rest periods.

2.3. Independent Component Analysis (ICA)

A group of spatial ICA was performed on preprocessed data using the Group ICA of fMRI

Toolbox [GIFT3.0a; http://icatb.sourceforge.net] as described elsewhere (Sambataro et al.,

2010). ICA decomposition was performed using the Infomax algorithm and resulted in 75

independent components (ICs) consisting of group spatial maps of IC loadings and related

time courses (TC), which were included in the mixing matrix. Group estimated independent

components were then back-reconstructed to individual subject IC maps using double

regression approach (Beckmann et al., 2009). Individual subject TCs were scaled using the

maximum intensity values, whereas IC maps were calibrated using the standard deviation of

the time courses. For each participant, an IC spatial map includes voxel-wise IC loadings that

represent local strength of FC and reflect the correspondence between the estimated TC in

each voxel for each individual and the average TC of the aggregate network itself. All the IC

maps were screened for reliability as indicated by a coefficient of stability (Iq) greater than

0.80 calculated by 50 bootstrapped permutated estimations of the ICs (ICASSO) and for

artifactual patterns defined by those IC maps with a spatial correlation $R^2 \geq 0.02$ with white

matter, $R^2 \geq 0.05$ for CSF and $R^2 \leq 0.005$ with gray matter were removed from the analysis.

Additionally, they were inspected for known vascular, ventricular, motion and susceptibility

artifact (Allen et al., 2011). This screening resulted in 34 INs (for a detailed description of the

INs and their spatial maps see Figure S.7-S.11 and Table S.1).

2.4. Statistical Analyses

We followed the same pipeline as described previously (Allen et al., 2011) for our statistical

analysis: First, we estimated three types of feature for each of the 34 INs for each subject

and created three group response matrices concatenated across all subjects (one for each

feature type); Second, we analyzed the response matrices using a multivariate approach

with backward selection of significant predictors followed by univariate tests.

2.4.1. Feature estimation. For each IN, we analyzed three types of features: IN spatial maps, TC spectra and pairwise between-INs functional network connectivity correlations (FNC).

A) Each spatial map was thresholded with t> mean + 4 standard deviations to select the most representative voxels according to the normal-gamma-gamma mixture model that fits these data (Allen et al., 2011);

B) Spectra were analyzed on detrended TCs (after mean, slope, and π and 2π period sines and cosines removal to avoid skewing in the averaging of the tapers) using the multitaper method as implemented in Chronux in MATLAB (http://www.*chronux*.org) with the time-bandwidth product set to three and the number of tapers set to five. Each spectrum was divided in 150 bins and log-transformed.

C) A 34 x 34 FNC matrix was calculated using Pearson's bivariate correlation between each pair of TCs. For each subject, TCs were detrended, despiked using the median absolute deviation as in 3Ddespike (https://afni.nimh.nih.gov/pub/dist/doc/program_help/3dDespike.html) and low-pass filtered (fifth-order Butterworth with high frequency cut-off=0.15 Hz). Correlation coefficients were then z-transformed using Fisher's transformation and entered a 34x34 symmetric cross-correlation matrix for each subject.

For each subject, 34 spatial maps, 34 spectra and a single 34x34 matrix of FNC were calculated. These features were modeled as separate vectors and concatenated per subject thus resulting in separate response matrices per feature type. A principal component analysis was then applied to concatenated response matrices to reduce the dimensionality and the autocorrelation of the data to 10 dimensions for each feature. Dimension-reduced features were then analyzed using multivariate analyses.

2.4.2. Multivariate and univariate analyses. We used a novel multivariate model selection strategy to reduce the number of statistical tests to be performed and to test the effects of specific predictors on a design matrix (Allen et al., 2011). First, we created a design matrix that included all the predictors: variables of interest [diagnosis (healthy controls, patients with MDD), paradigm (rest, task) and diagnosis by paradigm interaction] along with the nuisance variables (age, gender, head motion estimate, spatial normalization estimate, gray matter content, see Supplemental Information). Normalized nuisance variables were included to correct for the possible effects of demographic, structural or scan-related differences across subjects. Second, each separate response matrix was analyzed using a one-way multivariate analyses of covariance (MANCOVA) to identify significant predictors within the design matrix for using the MANCOVAN toolbox implemented in GIFT 3.0 (http://mialab.mrn.org/software/mancovan/index.html) which runs on MATLAB (the scripts used to analyze these data are available from the corresponding author upon request). Briefly, backward multivariate stepwise regressions are performed for each response matrix separately. For each IN c, the full MANCOVA model is $RM_c=DB+E$, where RM_c is the response matrix for the IN c, D is the design matrix, B the matrix of regression coefficients, and E the error matrix. At each step the full model is compared with a reduced model, obtained removing one predictor and its interactions (when available) from D, using a Wilk's lambda likelihood ratio test statistics. Then, the predictor associated with the least significant model across all the reduced models is removed, and reduced model becomes the full model for the subsequent regression until all predictors have been tested. The final reduced model (see Table S.1 for details on the degrees of freedom of each regression) includes only those predictors that are significant after correction for multiple comparisons using a false discovery rate approach [FDR (Genovese et al., 2002)] with $\alpha=0.05$. Following MANCOVA analyses, we performed univariate tests on the final reduced model applied to the original (not-dimension reduced) feature matrices separately to identify the

11

effects of diagnosis, paradigm, and diagnosis by paradigm on the spatial maps, the spectra and temporal correlations (FNC) for each IN. Partial correlation coefficients for each predictor were calculated from linear regressions with the feature matrix as a dependent variable while covarying out the effects of the other predictors. All tests were corrected for multiple comparisons using a level of α=0.05 FDR-corrected (see supplementary materials for degree of freedom). For the spatial maps, significant clusters were identified using an uncorrected voxel-wise threshold of p<0.001. To correct for multiple comparisons with a family-wise error rate at p<0.05, a minimum cluster size was estimated for the whole brain for each IC using 10'000 iterations of a Monte Carlo simulation implemented in 3dClustsim (http://afni.nimh.nih.gov/pub/dist/doc/program_help/3dClustSim.html; compile date: September 28, 2016). All coordinates are reported in the Montreal Neurological Institute (MNI) system.

3. Results

We found 34 reliable INs. Multivariate analyses yielded significant differences for the effects of diagnosis, paradigm, and diagnosis by paradigm in the spatial maps and in the spectra. Spatial maps showed an effect of diagnosis in three INs including the EN, the DMN and the DAN (Figure 1.A). The EN included prefronto-parietal regions predominantly on the left hemisphere. The DMN spanned across two INs: A more dorsal DMN (Figure 1.B, top) including posterior cingulate cortex (PCC), bilateral inferior parietal cortex, the hippocampus and medial prefrontal cortex (PFC); a more ventral DMN component (Figure 1.B, bottom) spanning across the hippocampus and the parahippocampus. The DAN (Figure 1.C) entailed bilateral superior parietal cortex. To identify voxel-wise differences between diagnostic groups across INs, a composite map was estimated. Maximum statistical difference for the effect of diagnosis at each voxel was calculated for each significant IN (Figure 2.A). Patients showed reduced connectivity in the PCC, bilateral superior parietal cortex, and anterior

hippocampus along with increased connectivity in the precuneus. More specifically, univariate post-hoc analyses revealed reduced connectivity in patients in left dorsolateral PFC (x,y,z = -45, 27, 45; k=87 ; Z=4.80; Figure 2.B) within the EN; within the ventral DMN, patients had reduced connectivity in the left parahippocampus (x,y,z = -42, -6, -45; k=141 ; Z=4.24; Figure 2.C); within the dorsal DMN , we found reduced connectivity (Figure 2.D left) in patients in left temporo-parietal cortex (x,y,z = -48, -75, 21; k=101; Z=4.17) and left PCC (x,y,z= -6, -63, 15; k=185 ; Z=4.82) along with increased connectivity in the left precuneus (x,y,z= -15, -78, 33; k=115 ; Z=4.59; Figure 2.D right). Within the DAN, no region survived to univariate correction for multiple comparisons.

Spectral analyses revealed reduced amplitude of LFO (0.04<f<0.08 Hz) in patients relative to controls in two INs: the left motor network (IN2, Figure 3.A) and the DAN (IN38, Figure 3.B) in patients relative to normal controls. The left motor network included mainly pre- and post-central gyrus, anterior cingulate and cerebellum (Figure S.11). The DAN (IN38) encompassed bilateral superior parietal lobule, intraparietal sulcus, frontal eye fields, posterior cingulate and left visual cortex (Figure S.11). Additionally, patients had increased high frequency spectral power of the left motor network. High frequency oscillations are thought to be artefactual by nature and not to arise from the gray matter (Zuo et al., 2010).

We also found a diagnosis by paradigm (rest vs. task) interaction (Figure 4.A) in the salience network that included bilateral insula and ventrolateral PFC (IN64, see Figure S.7 for the spatial map). Patients had greater LFO amplitude (0.04<f<0.08 Hz) during task performance relative to rest when compared to normal controls (Figure 4.B) but not in the other frequency bins.

Age, gender, motion, grey matter volume and warping had an effect on the spatial maps along with the spectra (Figure S.2). We did not find any significant effect of diagnosis or diagnosis by paradigm (rest vs task) on FNC. Age, motion and gray matter content had an effect on FNC correlations (Figure S.3). The paradigm modulated the spatial maps (Figure

S.4), the spectra (Figure S.5) and the FNC correlations (Figure S.6). In particular, following the

trial presentation frequency of one trial each 7.5 ± 0.5 seconds (Späti et al., 2014), the

spectral power was significantly greater at 0.13 Hz during task relative to rest condition (see

peaks in Figure 3.A, 3.B, and 4).

4. Discussion

The aim of the present study was to investigate altered dynamics of functional brain

networks in MDD at rest and during task performance. Our results show that the spatial

extent of the DMN and the EN were altered in patients with MDD compared to healthy

controls. In addition, the left motor and the DAN showed reduced power in the low-

frequency range in patients with MDD compared to healthy controls. These spatial and

temporal abnormalities were present in patients during both paradigms (rest and task),

whereas a diagnosis by paradigm interaction on the spectrum of network oscillations was

found in the salience network: patients had greater power amplitude in the low frequency

range during task relative to rest compared to normal controls.

In the present study, altered functional connectivity in the DMN was present across

two INs: A 'dorsal' component including the PCC, the inferior parietal cortex and the medial

PFC, and a 'ventral' component comprising the hippocampus and parahippocampus

bilaterally (Allen et al., 2011; Andrews-Hanna et al., 2014; Sambataro et al., 2013).

Compared to healthy controls, unmedicated patients with MDD showed altered connectivity

in the posterior regions of the DMN. Specifically, connectivity was decreased in the left

parahippocampus within the ventral component, and in the left temporal-parietal cortex

and the PCC within the dorsal component in patients with MDD. Conversely, they had

increased connectivity in the precuneus within the dorsal component. Reduced FC with the

PCC has been previously reported in first-episode medication naïve patients with MDD (Zhu

et al., 2012). A recent study investigating the FC of distinct DMN subsystems at-rest also showed abnormal FC with the PCC, the temporal-parietal cortex and the hippocampal formation in patients with MDD (Sambataro et al., 2013). Moreover, reduced suppression of the PCC (and the medial PFC) has also been found in patients with MDD performing an emotional task (Grimm et al., 2009). The importance of functional DMN abnormalities in temporal lobe regions is also supported by the results of Zeng and coworkers (2012) who used multivariate pattern analysis to discriminate medication-naïve patients with MDD from healthy controls. In this study, they found that the functional connections with high discriminative power were located in the DMN and included the bilateral hippocampus/parahippocampal gyrus, and the inferior temporal cortex (Zeng et al., 2012). Similarly, altered activity in the posterior DMN was confirmed by two recent meta-analyses of RS-fMRI data in MDD (Kaiser et al., 2015; Sundermann et al., 2014), but findings from task-based neuroimaging studies showed poor spatial overlap with findings from RS-fMRI studies (Sundermann et al., 2014). A possible explanation for the discrepancy between task- and RS-fMRI results may be related to the different measures that are investigated in these studies and specifically task induced activations and FC, respectively. Our results confirm and extend these previous findings by showing that functional abnormalities within the posterior DMN in unmedicated patients with MDD are prominent both at rest and during task performance.

The PCC is considered one of the hubs of the DMN with a general role in attention modulation, and in episodic and working memory (Buckner et al., 2008). The temporal cortex, the hippocampus and parahippocampus regions have a specific role in memory processes (Buckner et al., 2008). It is, therefore, possible that functional abnormalities in these regions contribute to memory impairments, as consistently reported in MDD (Drevets et al., 2008). Patients showed also altered FC with the precuneus, a finding consistent with previous studies in MDD (Greicius et al., 2007; Sheline et al., 2009; Zhu et al., 2012). In

contrast to the decreased FC found with the temporal DMN regions, patients showed

increased connectivity with the precuneus. This functional dissociation is in line with

anatomical evidence showing clear differences in terms of anatomical connections and

cytoarchitecture between the PCC and the precuneus (Buckwalter et al., 2008). The

precuneus is considered important during self-perception, internal mentation, and memory

retrieval (Cavanna and Trimble, 2006; Gusnard et al., 2001; Lundstrom et al., 2005), thus

increased precuneus connectivity may be related to increased self-referential processing in

MDD (Sheline et al., 2009), or represents a compensatory process for memory deficits

associated with other DMN regions. Interestingly, increased precuneus and decreased PCC

connectivity has been reported also in schizophrenia (Sambataro et al., 2010). Although

altered memory and self-referential processes have also been reported in schizophrenic

patients, there are important distinctions between the two disorders (Egeland et al., 2003;

Kuhn and Gallinat, 2013). It is possible that increased precuneus connectivity represents a

more general compensatory effect related to reduced PCC function, a hypothesis that needs

to be further investigated.

In addition to the DMN, patients with depression showed decreased FC with the

right dorsolateral PFC (DLPFC) in the EN. Abnormal DLPFC response has been reported

during a variety of emotional and cognitive tasks in patients with MDD (Diener et al., 2012)

and abnormal FC of the DLPFC has been found in MDD patients during working memory

(Vasic et al., 2009). More importantly, the DLPFC has been shown to play a key role in

regulating DMN activity. Using transcranial magnetic stimulation in healthy subjects, Chen *et

al.* (2013) were able to demonstrate that stimulation of the DLPFC suppresses the DMN,

whereas inhibition had opposite effects (Chen et al., 2013). These results strongly suggest an

important role of the interplay between the EN and the DMN that is thought to be mediated

by the salience network (Chand and Dhamala, 2016), which showed also altered FC in MDD

(see below). The altered modulation of EN and DMN may be highly relevant to MDD

pathogenesis, since impaired DMN suppression and increased self-referential processing have been proposed to play a crucial role in the development and the maintenance of a major depressive episode (Hamilton et al., 2011; Marchetti et al., 2012; Northoff et al., 2011; Pizzagalli, 2011).

MDD was associated with changes in the LFO amplitude during task and at rest in multiple networks, including salience, motor and dorsal attention networks. Recent studies in MDD show changes in amplitude of low frequency oscillations in various brain regions at-rest (Liu et al., 2013; Sambataro et al., 2010; Wang et al., 2012a; Wang et al., 2016; Zhang et al., 2014). These oscillations can be modulated by the performance of different types of task, including visual stimulation (Leopold et al., 2003), working memory (Balsters et al., 2013), and language processing (Lohmann et al., 2010). Furthermore, the amplitude of LFO predicts task performance at cognitive (Balsters et al., 2013) as well as sensory detection tasks (Monto et al., 2008). We found that in the salience network patients with MDD had increased power of the LFO during task performance relative to rest. Conversely, normal subjects had reduced power during rest compared to task performance. The salience network comprised the right anterior insula (AI)/ventrolateral PFC and to a lower extent also the left AI. Increased amplitude of LFOs at-rest in the AI has recently been found in MDD (Zhang et al., 2014). Moreover, functional and structural abnormalities in the fronto-insular cortex have been consistently reported in patients with MDD (Sprengelmeyer et al., 2011; Veer et al., 2010). Importantly, the right AI is considered to play a major role in switching between the DMN and the EN when a salient event occurs (Sridharan et al., 2008), thus increased LFOs amplitude in the salience network during task performance relative to rest in patients compared to controls may contribute to the abnormal network's switching function in MDD (see before). This interpretation is supported by evidence from a recent study that specifically compared the functional 'dominance' of the DMN over the EN at-rest in patients with MDD and healthy controls (Hamilton et al., 2011). While healthy participants exhibited

greater response in the right fronto-insular cortex at the onset of increase in DMN activity, patients with MDD showed greater fronto-insular activity at the onset of increase in EN activity, suggesting an abnormal functional activation of the right fronto-insular cortex specifically during network switching. Interestingly, we found a diagnosis by task effect only on the $0.04<f<0.08$ Hz range of LFOs of the salience network but not in the lower bands. The difference in the neurobiology and the functional implication underlying different frequency bands within the LFOs remain unknown. Previous reports have shown differential representation of the low frequency oscillations based on the brain regions (Wang et al., 2016). Indeed, Wang and coworkers found a greater representation of $0.04<f<0.08$ Hz LFOs in bilateral insula relative to other cortical regions. The amplitude of the low frequency in the DAN and the left motor networks were also altered in patients with MDD at rest and during task performance. The DAN encompassed bilateral superior parietal lobule, intraparietal sulcus, frontal eye fields, posterior cingulate and left visual cortex, whereas the left motor network included the pre- and post-central gyrus, anterior cingulate and cerebellum. Previous findings in unmedicated MDD showed altered amplitude of LFO in brain regions of the DAN and motor networks (Wang et al., 2012a). Furthermore, reduced FC of the DAN was found also in a recent meta-analysis of RS-fMRI data in MDD (Kaiser et al., 2015). Reduced connectivity of the motor pathways (Bracht et al., 2012) has been reported in patients with MDD. LFOs are thought to originate from the cortical modulation of neuronal excitability within large-scale networks (Pan et al., 2013). Thus, lower LFOs at rest as well as during task performance can be interpreted as reflecting altered activity of the whole DAN and the motor networks. Given the role of the DAN in orienting attention based on internal goals (goal-driven) (Corbetta et al., 2008), its reduced connectivity may contribute to the limited engagement with the external environment and potentially to increased self-reflection in MDD. Also, alterations in sensory-motor pathways can contribute

to mood regulation and the risk for MDD onset (Canbeyli, 2010) as well as to fatigue and other the psychomotor symptoms.

Some limitations of this study need to be acknowledged. First, the type of statistical analysis and the sample size limit the power of the study. To control for several sources of bias on neuroimaging studies, we used a multivariate analysis approach that partials out the effect of nuisance variables including demographics, preprocessing differences, and structural variability, while allowing a robust control for the number of multiple comparisons. A MANCOVA analysis, when including a large number of nuisance covariates, results in reduced degrees of freedom, and ultimately in lower power to detect a significant effect thus potentially increasing the rate of false negative results. Furthermore, a small sample size (n=38), although in line with recent studies using the same MANCOVA approach in psychiatric disorders (Caminiti et al., 2015; van Belle et al., 2015), may overestimate the effect size thus increasing the risk of number of false positive results (for more details, see Bacchetti, 2013; Button et al., 2013; Quinlan, 2013). Hence, future larger replication studies are warranted to validate the reproducibility of these results. Second, patients with MDD with comorbid anxiety disorders were included in the study. While anxiety could also contribute to these findings, the comorbidity rate of these disorders is about 60-70%, thus making this sample more representative of the general population of the patients with MDD (Kessler et al., 1996). Third, groups were matched for behavioral performances for the whole task as well as for the first part that we included in the analyses. However, qualitative differences may still be present in the second part of the task potentially biasing connectivity measures during task performance. Nonetheless, as the rationale of including different paradigms was to study whether alterations of INs persisted during task and most of them occurred both at-rest and during task, we believe that qualitative difference, if present, had limited impact on our findings. Furthermore, to avoid the temporal design of task to bias the

spectral analyses in the LFOs, we used a task with a frequency of trial presentation above this range.

Overall, the findings of our study indicate that alterations in the brain dynamics of the DMN, the EN, and dorsal attentional and motor networks in MDD are persistent across rest and task performance, thus supporting an important role of these networks in MDD. Additionally, the dynamics of the salience network was affected by the paradigm, thus indicating an altered process-dependent modulation of this network in MDD that could be targeted by cognitive rehabilitation. Notably, network changes could not be unduly driven by pharmacological treatment as our patients were unmedicated. These changes may be used as neural phenotypes to investigate the pathophysiology of MDD and as possible targets for pharmacological treatments. Future studies investigating these alterations in unaffected relatives of patients and their ability to classify patients with MDD relative to healthy controls are warranted.

Conflict of interest: All other authors have no conflict of interest to report.

Author's contributions: FS and SS designed the experiment. FS and EV analyzed the data. ND and JB conducted the experiments. FS, SS, MgH and ES contributed to interpretation of the data. FS and SS wrote the manuscript with input from all the authors. All authors approved the final manuscript.

References

Allen, E.A., Erhardt, E.B., Damaraju, E., Gruner, W., Segall, J.M., Silva, R.F., Havlicek, M., Rachakonda, S., Fries, J., Kalyanam, R., Michael, A.M., Caprihan, A., Turner, J.A., Eichele, T., Adelsheim, S., Bryan, A.D., Bustillo, J., Clark, V.P., Feldstein Ewing, S.W., Filbey, F., Ford, C.C., Hutchison, K., Jung, R.E., Kiehl, K.A., Kodituwakku, P., Komesu, Y.M., Mayer, A.R., Pearlson, G.D., Phillips, J.P., Sadek, J.R., Stevens, M., Teuscher, U., Thoma, R.J., Calhoun, V.D., 2011. A baseline for the multivariate comparison of resting-state networks. Front Syst Neurosci 5, 2.
Andrews-Hanna, J.R., Smallwood, J., Spreng, R.N., 2014. The default network and self-generated thought: component processes, dynamic control, and clinical relevance. Ann N Y Acad Sci 1316, 29-52.
Bacchetti, P., 2013. Small sample size is not the real problem. Nat Rev Neurosci 14, 585.
Balsters, J.H., Robertson, I.H., Calhoun, V.D., 2013. BOLD Frequency Power Indexes Working Memory Performance. Front Hum Neurosci 7, 207.
Beckmann, C., Mackay, C., Filippini, N., Smith, S.M., 2009. Group comparison of resting-state FMRI data using multi-subject ICA and dual regression. Neuroimage 47, S148.
Biswal, B., Yetkin, F.Z., Haughton, V.M., Hyde, J.S., 1995. Functional connectivity in the motor cortex of resting human brain using echo-planar MRI. Magnetic resonance in medicine 34, 537-541.
Biswal, B.B., Mennes, M., Zuo, X.N., Gohel, S., Kelly, C., Smith, S.M., Beckmann, C.F., Adelstein, J.S., Buckner, R.L., Colcombe, S., Dogonowski, A.M., Ernst, M., Fair, D., Hampson, M., Hoptman, M.J., Hyde, J.S., Kiviniemi, V.J., Kotter, R., Li, S.J., Lin, C.P., Lowe, M.J., Mackay, C., Madden, D.J., Madsen, K.H., Margulies, D.S., Mayberg, H.S., McMahon, K., Monk, C.S., Mostofsky, S.H., Nagel, B.J., Pekar, J.J., Peltier, S.J., Petersen, S.E., Riedl, V., Rombouts, S.A., Rypma, B., Schlaggar, B.L., Schmidt, S., Seidler, R.D., Siegle, G.J., Sorg, C., Teng, G.J., Veijola, J., Villringer, A., Walter, M., Wang, L., Weng, X.C., Whitfield-Gabrieli, S., Williamson, P., Windischberger, C., Zang, Y.F., Zhang, H.Y., Castellanos, F.X., Milham, M.P., 2010. Toward discovery science of human brain function. Proc Natl Acad Sci U S A 107, 4734-4739.
Bracht, T., Federspiel, A., Schnell, S., Horn, H., Hofle, O., Wiest, R., Dierks, T., Strik, W., Muller, T.J., Walther, S., 2012. Cortico-cortical white matter motor pathway microstructure is related to psychomotor retardation in major depressive disorder. PLoS One 7, e52238.
Buckner, R.L., Andrews-Hanna, J.R., Schacter, D.L., 2008. The brain's default network: anatomy, function, and relevance to disease. Ann N Y Acad Sci 1124, 1-38.
Buckwalter, J.A., Parvizi, J., Morecraft, R.J., van Hoesen, G.W., 2008. Thalamic projections to the posteromedial cortex in the macaque. J Comp Neurol 507, 1709-1733.
Button, K.S., Ioannidis, J.P., Mokrysz, C., Nosek, B.A., Flint, J., Robinson, E.S., Munafo, M.R., 2013. Power failure: why small sample size undermines the reliability of neuroscience. Nat Rev Neurosci 14, 365-376.
Buzsaki, G., Draguhn, A., 2004. Neuronal oscillations in cortical networks. Science 304, 1926-1929.
Calhoun, V.D., Adali, T., Pearlson, G.D., Pekar, J.J., 2001. A method for making group inferences from functional MRI data using independent component analysis. Hum Brain Mapp 14, 140-151.
Caminiti, S.P., Canessa, N., Cerami, C., Dodich, A., Crespi, C., Iannaccone, S., Marcone, A., Falini, A., Cappa, S.F., 2015. Affective mentalizing and brain activity at rest in the behavioral variant of frontotemporal dementia. NeuroImage. Clinical 9, 484-497.
Canbeyli, R., 2010. Sensorimotor modulation of mood and depression: an integrative review. Behav Brain Res 207, 249-264.
Cavanna, A.E., Trimble, M.R., 2006. The precuneus: a review of its functional anatomy and behavioural correlates. Brain 129, 564-583.

Chand, G.B., Dhamala, M., 2016. Interactions Among the Brain Default-Mode, Salience, and Central-Executive Networks During Perceptual Decision-Making of Moving Dots. Brain connectivity 6, 249-254.

Chen, A.C., Oathes, D.J., Chang, C., Bradley, T., Zhou, Z.W., Williams, L.M., Glover, G.H., Deisseroth, K., Etkin, A., 2013. Causal interactions between fronto-parietal central executive and default-mode networks in humans. Proc Natl Acad Sci U S A.

Cole, D.M., Smith, S.M., Beckmann, C.F., 2010. Advances and pitfalls in the analysis and interpretation of resting-state FMRI data. Front Syst Neurosci 4, 8.

Corbetta, M., Patel, G., Shulman, G.L., 2008. The reorienting system of the human brain: from environment to theory of mind. Neuron 58, 306-324.

DeRubeis, R.J., Siegle, G.J., Hollon, S.D., 2008. Cognitive therapy versus medication for depression: treatment outcomes and neural mechanisms. Nat Rev Neurosci 9, 788-796.

Diener, C., Kuehner, C., Brusniak, W., Ubl, B., Wessa, M., Flor, H., 2012. A meta-analysis of neurofunctional imaging studies of emotion and cognition in major depression. Neuroimage 61, 677-685.

Drevets, W.C., Price, J.L., Furey, M.L., 2008. Brain structural and functional abnormalities in mood disorders: implications for neurocircuitry models of depression. Brain Struct Funct 213, 93-118.

Egeland, J., Sundet, K., Rund, B.R., Asbjornsen, A., Hugdahl, K., Landro, N.I., Lund, A., Roness, A., Stordal, K.I., 2003. Sensitivity and specificity of memory dysfunction in schizophrenia: a comparison with major depression. J Clin Exp Neuropsychol 25, 79-93.

Fox, M.D., Raichle, M.E., 2007. Spontaneous fluctuations in brain activity observed with functional magnetic resonance imaging. Nat Rev Neurosci 8, 700-711.

Graham, J., Salimi-Khorshidi, G., Hagan, C., Walsh, N., Goodyer, I., Lennox, B., Suckling, J., 2013. Meta-analytic evidence for neuroimaging models of depression: State or trait? J Affect Disord 151, 423-431.

Greicius, M.D., Flores, B.H., Menon, V., Glover, G.H., Solvason, H.B., Kenna, H., Reiss, A.L., Schatzberg, A.F., 2007. Resting-state functional connectivity in major depression: abnormally increased contributions from subgenual cingulate cortex and thalamus. Biol Psychiatry 62, 429-437.

Grimm, S., Boesiger, P., Beck, J., Schuepbach, D., Bermpohl, F., Walter, M., Ernst, J., Hell, D., Boeker, H., Northoff, G., 2009. Altered negative BOLD responses in the default-mode network during emotion processing in depressed subjects. Neuropsychopharmacology 34, 932-932.

Guo, W.B., Liu, F., Xue, Z.M., Xu, X.J., Wu, R.R., Ma, C.Q., Wooderson, S.C., Tan, C.L., Sun, X.L., Chen, J.D., Liu, Z.N., Xiao, C.Q., Chen, H.F., Zhao, J.P., 2012. Alterations of the amplitude of low-frequency fluctuations in treatment-resistant and treatment-response depression: a resting-state fMRI study. Prog Neuropsychopharmacol Biol Psychiatry 37, 153-160.

Gusnard, D.A., Akbudak, E., Shulman, G.L., Raichle, M.E., 2001. Medial prefrontal cortex and self-referential mental activity: relation to a default mode of brain function. Proc Natl Acad Sci U S A 98, 4259-4264.

Hamilton, J.P., Furman, D.J., Chang, C., Thomason, M.E., Dennis, E., Gotlib, I.H., 2011. Default-mode and task-positive network activity in major depressive disorder: implications for adaptive and maladaptive rumination. Biol Psychiatry 70, 327-333.

Kaiser, R.H., Andrews-Hanna, J.R., Wager, T.D., Pizzagalli, D.A., 2015. Large-Scale Network Dysfunction in Major Depressive Disorder: A Meta-analysis of Resting-State Functional Connectivity. JAMA Psychiatry 72, 603-611.

Kessler, R.C., Nelson, C.B., McGonagle, K.A., Liu, J., Swartz, M., Blazer, D.G., 1996. Comorbidity of DSM-III-R major depressive disorder in the general population: results from the US National Comorbidity Survey. The British journal of psychiatry. Supplement, 17-30.

Kuhn, S., Gallinat, J., 2013. Resting-state brain activity in schizophrenia and major depression: a quantitative meta-analysis. Schizophr Bull 39, 358-365.

Leopold, D.A., Murayama, Y., Logothetis, N.K., 2003. Very slow activity fluctuations in monkey visual cortex: implications for functional brain imaging. Cereb Cortex 13, 422-433.

Liberg, B., Rahm, C., 2015. The functional anatomy of psychomotor disturbances in major depressive disorder. Frontiers in psychiatry 6, 34.

Liu, F., Guo, W., Liu, L., Long, Z., Ma, C., Xue, Z., Wang, Y., Li, J., Hu, M., Zhang, J., Du, H., Zeng, L., Liu, Z., Wooderson, S.C., Tan, C., Zhao, J., Chen, H., 2013. Abnormal amplitude low-frequency oscillations in medication-naive, first-episode patients with major depressive disorder: a resting-state fMRI study. J Affect Disord 146, 401-406.

Logothetis, N.K., Murayama, Y., Augath, M., Steffen, T., Werner, J., Oeltermann, A., 2009. How not to study spontaneous activity. Neuroimage 45, 1080-1089.

Lohmann, G., Hoehl, S., Brauer, J., Danielmeier, C., Bornkessel-Schlesewsky, I., Bahlmann, J., Turner, R., Friederici, A., 2010. Setting the frame: the human brain activates a basic low-frequency network for language processing. Cereb Cortex 20, 1286-1292.

Lundstrom, B.N., Ingvar, M., Petersson, K.M., 2005. The role of precuneus and left inferior frontal cortex during source memory episodic retrieval. Neuroimage 27, 824-834.

Marchetti, I., Koster, E.H., Sonuga-Barke, E.J., De Raedt, R., 2012. The default mode network and recurrent depression: a neurobiological model of cognitive risk factors. Neuropsychol Rev 22, 229-251.

Monto, S., Palva, S., Voipio, J., Palva, J.M., 2008. Very slow EEG fluctuations predict the dynamics of stimulus detection and oscillation amplitudes in humans. J Neurosci 28, 8268-8272.

Northoff, G., Duncan, N.W., Hayes, D.J., 2010. The brain and its resting state activity--experimental and methodological implications. Prog Neurobiol 92, 593-600.

Northoff, G., Wiebking, C., Feinberg, T., Panksepp, J., 2011. The 'resting-state hypothesis' of major depressive disorder-a translational subcortical-cortical framework for a system disorder. Neurosci Biobehav Rev 35, 1929-1945.

Pan, W.J., Thompson, G.J., Magnuson, M.E., Jaeger, D., Keilholz, S., 2013. Infraslow LFP correlates to resting-state fMRI BOLD signals. Neuroimage 74, 288-297.

Pandya, M., Altinay, M., Malone, D.A., Jr., Anand, A., 2012. Where in the brain is depression? Curr Psychiatry Rep 14, 634-642.

Pizzagalli, D.A., 2011. Frontocingulate dysfunction in depression: toward biomarkers of treatment response. Neuropsychopharmacology 36, 183-206.

Quinlan, P.T., 2013. Misuse of power: in defence of small-scale science. Nat Rev Neurosci 14, 585.

Raichle, M.E., Snyder, A.Z., 2007. A default mode of brain function: a brief history of an evolving idea. Neuroimage 37, 1083-1090; discussion 1097-1089.

Roiser, J.P., Elliott, R., Sahakian, B.J., 2012. Cognitive mechanisms of treatment in depression. Neuropsychopharmacology 37, 117-136.

Sambataro, F., Blasi, G., Fazio, L., Caforio, G., Taurisano, P., Romano, R., Di Giorgio, A., Gelao, B., Lo Bianco, L., Papazacharias, A., Popolizio, T., Nardini, M., Bertolino, A., 2010. Treatment with olanzapine is associated with modulation of the default mode network in patients with Schizophrenia. Neuropsychopharmacology 35, 904-912.

Sambataro, F., Wolf, N.D., Pennuto, M., Vasic, N., Wolf, R.C., 2013. Revisiting default mode network function in major depression: evidence for disrupted subsystem connectivity. Psychol Med, 1-11.

Seeley, W.W., Menon, V., Schatzberg, A.F., Keller, J., Glover, G.H., Kenna, H., Reiss, A.L., Greicius, M.D., 2007. Dissociable intrinsic connectivity networks for salience processing and executive control. J Neurosci 27, 2349-2356.

Sheline, Y.I., Barch, D.M., Price, J.L., Rundle, M.M., Vaishnavi, S.N., Snyder, A.Z., Mintun, M.A., Wang, S., Coalson, R.S., Raichle, M.E., 2009. The default mode network and self-referential processes in depression. Proc Natl Acad Sci U S A 106, 1942-1947.

Shi, H., Wang, X., Yi, J., Zhu, X., Zhang, X., Yang, J., Yao, S., 2015. Default mode network alterations during implicit emotional faces processing in first-episode, treatment-naive major depression patients. Front Psychol 6, 1198.

Späti, J., Chumbley, J., Brakowski, J., Dorig, N., Grosse Holtforth, M., Seifritz, E., Spinelli, S., 2014. Functional lateralization of the anterior insula during feedback processing. Hum Brain Mapp.

Sprengelmeyer, R., Steele, J.D., Mwangi, B., Kumar, P., Christmas, D., Milders, M., Matthews, K., 2011. The insular cortex and the neuroanatomy of major depression. J Affect Disord 133, 120-127.

Sridharan, D., Levitin, D.J., Menon, V., 2008. A critical role for the right fronto-insular cortex in switching between central-executive and default-mode networks. Proc Natl Acad Sci U S A 105, 12569-12574.

Sundermann, B., Olde Lutke Beverborg, M., Pfleiderer, B., 2014. Toward literature-based feature selection for diagnostic classification: a meta-analysis of resting-state fMRI in depression. Front Hum Neurosci 8, 692.

van Belle, J., van Raalten, T., Bos, D.J., Zandbelt, B.B., Oranje, B., Durston, S., 2015. Capturing the dynamics of response variability in the brain in ADHD. NeuroImage. Clinical 7, 132-141.

Vasic, N., Walter, H., Sambataro, F., Wolf, R.C., 2009. Aberrant functional connectivity of dorsolateral prefrontal and cingulate networks in patients with major depression during working memory processing. Psychol Med 39, 977-987.

Veer, I.M., Beckmann, C.F., van Tol, M.J., Ferrarini, L., Milles, J., Veltman, D.J., Aleman, A., van Buchem, M.A., van der Wee, N.J., Rombouts, S.A., 2010. Whole brain resting-state analysis reveals decreased functional connectivity in major depression. Front Syst Neurosci 4.

Wang, L., Dai, W., Su, Y., Wang, G., Tan, Y., Jin, Z., Zeng, Y., Yu, X., Chen, W., Wang, X., Si, T., 2012a. Amplitude of low-frequency oscillations in first-episode, treatment-naive patients with major depressive disorder: a resting-state functional MRI study. PLoS One 7, e48658.

Wang, L., Hermens, D.F., Hickie, I.B., Lagopoulos, J., 2012b. A systematic review of resting-state functional-MRI studies in major depression. J Affect Disord 142, 6-12.

Wang, L., Kong, Q., Li, K., Su, Y., Zeng, Y., Zhang, Q., Dai, W., Xia, M., Wang, G., Jin, Z., Yu, X., Si, T., 2016. Frequency-dependent changes in amplitude of low-frequency oscillations in depression: A resting-state fMRI study. Neurosci Lett 614, 105-111.

Zeng, L.L., Shen, H., Liu, L., Wang, L., Li, B., Fang, P., Zhou, Z., Li, Y., Hu, D., 2012. Identifying major depression using whole-brain functional connectivity: a multivariate pattern analysis. Brain 135, 1498-1507.

Zhang, X., Zhu, X., Wang, X., Zhong, M., Yi, J., Rao, H., Yao, S., 2014. First-episode medication-naive major depressive disorder is associated with altered resting brain function in the affective network. PLoS One 9, e85241.

Zhu, X., Wang, X., Xiao, J., Liao, J., Zhong, M., Wang, W., Yao, S., 2012. Evidence of a dissociation pattern in resting-state default mode network connectivity in first-episode, treatment-naive major depression patients. Biol Psychiatry 71, 611-617.

Zuo, X.N., Di Martino, A., Kelly, C., Shehzad, Z.E., Gee, D.G., Klein, D.F., Castellanos, F.X., Biswal, B.B., Milham, M.P., 2010. The oscillating brain: complex and reliable. Neuroimage 49, 1432-1445.

Figure Legends

Figure 1. Intrinsic networks (INs) showing a effect of diagnosis on spatial maps: A) the Executive network (IN 53), B) the default mode network (top, dorsal component, IN 56; bottom, ventral component, IN 9) and C) the dorsal attentional network (IN 38) showed significant changes between MDD and HC using a MANCOVA (Figure 2). One-sample t-test maps display the spatial pattern of the INs across of subjects and paradigms overlaid on the MNI brain template. Color bar indicates t-scores. MNI, Montreal Neurological Institute.

Figure 2. Spatial extent of reduced connectivity within the intrinsic networks (INs) in MDD. A) Multivariate analysis shows the brain voxels with different independent component (IC) loadings across all INs in HCs relative to MDD. Spatial maps of significantly increased IC loadings in patients with MDD relative to HCs within the B) Executive network (IN53), the C) ventral DMN (IN9) and the D) dorsal DMN (IN56). Maps of IN connectivity differences are thresholded at p=0.005 and corrected for multiple comparisons with alpha=0.05 and overlaid on the MNI brain template. Color bar indicates –sign(t)*log10(p) and t-scores for the HC>MDD comparison for multivariate and univariate analysis, respectively. Default Mode Network, DMN; HC, Healthy controls; MDD, Major Depressive Disorder; MNI, Montreal Neurological Institute.

Figure 3. Power differences of the intrinsic networks (INs) in MDD. MDD had reduced power in the low frequency spectrum for both the motor and the dorsal

attention network. Conversely, they had greater power in the high frequency domain in the motor IN. Power spectra of the A) motor (IN 2) and the B) dorsal attentional (IN 38) networks are indicated for each diagnosis (HC, MDD) and paradigm (rest and task). At the bottom of the spectra, two-sample t-tests of the diagnostic differences for the contrast MDD>HC per frequency bin of the power spectra (n=150) are reported for IN2 and IN38, respectively. Color bar indicates −sign(t)*log10(p) for the comparison MDD >HC. HC, Healthy controls; MDD, Major Depressive Disorder.

Figure 4. Diagnosis by paradigm interaction on power spectra of the intrinsic networks (INs). MDD had greater power amplitude in the low frequency during task compared to rest in the salience network relative to HC who, conversely, had greater power in the high frequency range during rest compared to task. A) Power spectra of salience network (IN 64) is indicated for each diagnosis and paradigm (rest and task); at the bottom of the spectrum, two-sample t-tests of the diagnostic differences for the interaction (MDD - HC) x (Rest – Task) per frequency bin of the power spectrum (n=150) are reported. B) Power spectra for each diagnostic group (left panel, HC; right panel, MDD) binned by 6 frequency ranges are reported for each paradigm (left, Rest; right Task). Frequency bands: very low frequency, <0.04 Hz (blue); low frequency, 0.04-0.08 Hz (red); medium frequency, 0.08-0.12 Hz (green); high frequency, 0.12-0-17 Hz (magenta); very high frequency, 0.17-0.21 Hz (black), 0.21-0.25 Hz (grey). Color bar indicates −sign(t)log10(p) for the interaction diagnosis by paradigm. HC, Healthy controls; MDD, Major Depressive Disorder.

Table 1. Demographics, symptom severity and behavioral information for healthy controls and patients with MDD.

	Patients with MDD N = 19	Healthy controls N = 19	Statistics
Gender (% Male)	26	42	$p > 0.3$
Age (years)*	33.5 ± 9.8	38.5 ± 12.4	$p > 0.1$
Education (years)*	16.1 ± 2.8	16.4 ± 2.7	$p > 0.8$
BDI-II*	25.8 ± 8.7	-	-
IDS*	33.8 ± 8.5	-	-
Single MDD episode	5	-	-
H Scale*	73.2 ± 11.6	43.4 ± 10.3	$t(36) = -8.4, p < 0.001$
STAI Trait*	31.9 ± 8.8	56.2 ± 11.2	$t(36) = -7.4, p < 0.001$
STAI State*	33.5 ± 6.1	44.9 ± 5.2	$t(36) = -6.3, p < 0.001$
Correct trials (%)*	67.6 ± 10.7	63.3 ± 9.9	$p > 0.2$
Miss (%)*	1.3 ± 1.9	1.1 ± 2.9	$p > 0.7$
RT correct (ms)*	554 ± 167	530 ± 101	$p > 0.6$
RT incorrect (ms)*	595 ± 142	573 ± 111	$p > 0.5$

* reported as mean ± SD.
P-values for between-group t-tests or chi-squared analyses are presented in the final column.
BDI-II, Beck Depression Inventory-II; IDS, Inventory of Depressive Symptomatology;
H Scale, Hopelessness scale; STAI, Spielberger Trait and State Anxiety Inventory;
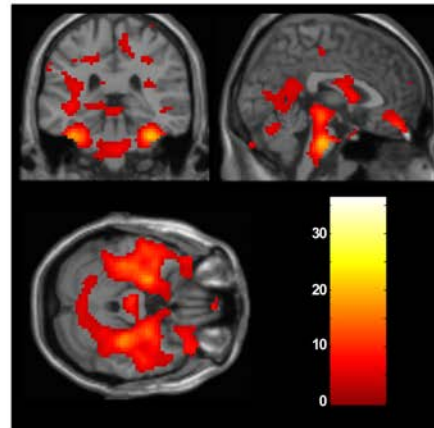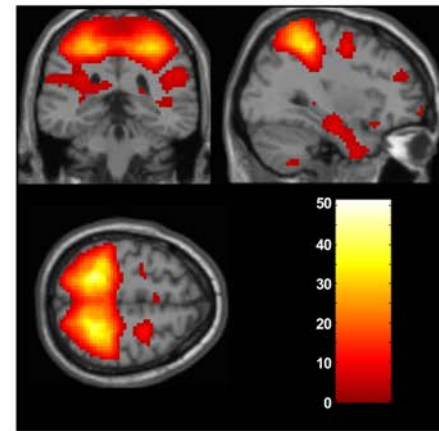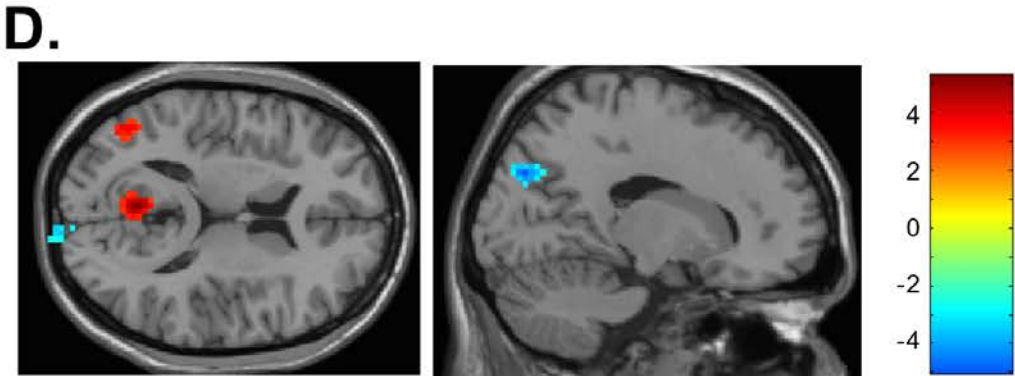RT, reaction time in milliseconds (ms)

Figure 1
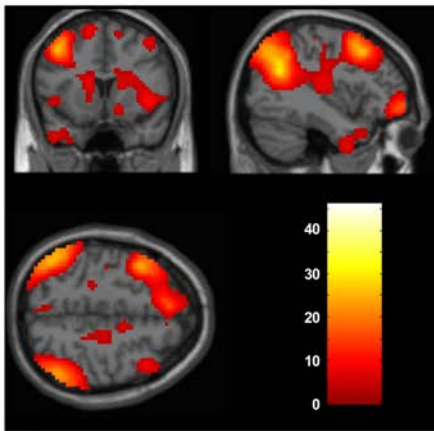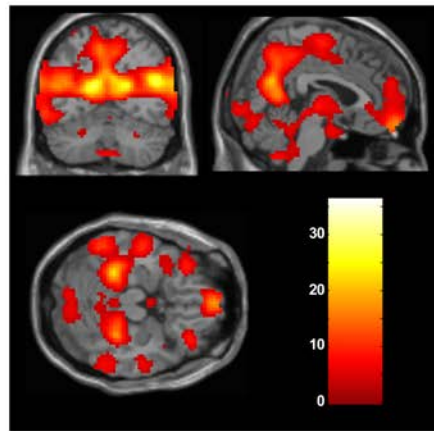
Figure 1

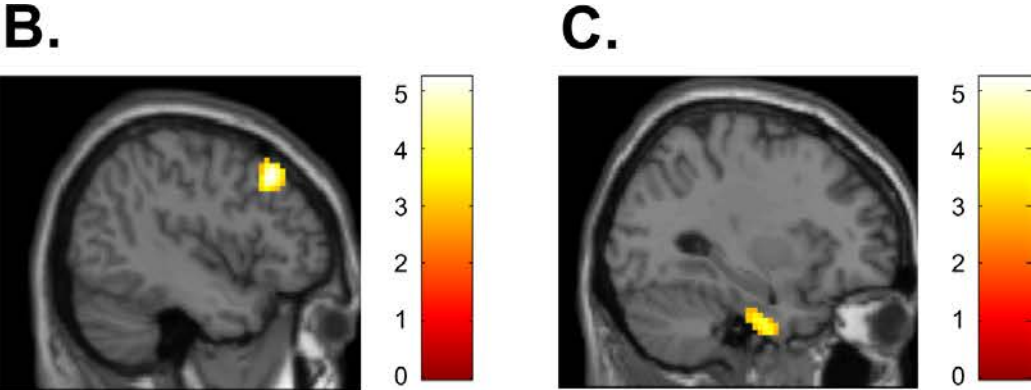# Figure 3

Figure 4